Adsorption Science & Technology

Research Article

Adsorption Science & Technology
2018, Vol. 36(3–4) 1178–1198

DOI: 10.1177/0263617418759776
journals.sagepub.com/home/adt
SAGE

The adsorption study of Royal Blue Tiafix and Black Tiassolan dyes using bone char as adsorbent

Rowander A Moura, Araceli A Seolatto, Maria E de Oliveira Ferreira and Fernanda F Freitas
Federal University of Goiás, Brazil

Abstract

In this study, the potential of bone char for Royal Blue Tiafix and Black Tiassolan dyes adsorption from aqueous solutions was evaluated. The adsorbent was characterized physically and chemically by adsorption/desorption of N_2 at 77 K, scanning electron microscopy, X-ray diffraction, and infrared spectroscopy. The equilibrium adsorption results for bone char can be successfully modeled by the Langmuir and Freundlich isotherms. Pseudo-first-order and pseudo-second-order models were used to describe the kinetic data and rate constants were evaluated. Kinetics of each dye was found to follow pseudo-second-order rate kinetic model, with great correlation (higher than 0.99). In order to reduce the number of experiments to achieve better dye removal efficiency, a 2^3 full factorial design with three central points and six axial points was applied in the equilibrium experiments. The variables analyzed were agitation, temperature, and pH.

Keywords

Factorial design, adsorbent, bone char, dye adsorption

Submission date: 10 August 2017; Acceptance date: 16 January 2018

Introduction

According to the United Nations World Water Development Report (2015) global water demand is strongly influenced by the population growth, the urbanization, the food and

Corresponding author:
Fernanda F Freitas, Institute of Chemistry, Federal University of Goiás, Goiânia CEP 74690-900, Goiás, Brazil.
Email: fernanda_ferreira_freitas@ufg.br

energy security policies, and the macroeconomic processes, such as the globalization of trade, changes in diet, and increased consumption. In 2050, an increase of 55% in global water demand is expected, mainly due to a demand increased from the industrial sector, thermoelectric power generation systems, and home users.

Regarding industrial development, among the various sectors, the textile industries have a prominent position. The sectors of activities such as yarn dyeing and industrial laundries generate large amounts of wastewater containing chemicals present in the industrial effluent. Typically, this wastewater is subjected to treatment at the wastewater treatment plant (WTP) of the companies themselves, becoming a solid waste, called sludge (Islam et al., 2011).

Textile industries have great difficulty in effectively treating wastewater generated in its complex production chain; particularly on removing dyes from these effluents, even in small quantities, given their intense color. In addition, there are the environmental impacts caused by the sludge generated by the textile industry effluent treatment, which in most cases do not have adequate treatment and disposal (Karthik and Rathinamoorthy, 2015). The final destination of sludge generated in WTPs is a serious problem worldwide (Tamanini et al., 2008).

Due to the low biodegradability of dyes, conventional processes of treating textile waste are not very efficient. Therefore, the type of treatment used to remove the dye may involve physical or chemical processes such as coagulation, flocculation, advanced oxidation (H_2O_2/UV), ozonation, ion exchange, irradiation, and adsorption (Belhouchat et al., 2017; Luo et al., 2010). Among these, adsorption has proven to be one of the most effective methods due to its simplicity and high efficiency (Cheng et al., 2015; Marrakchi et al., 2017), with advantages like, in some cases, the possibility of recovery of the dye, in concentrated form, and of the adsorbent.

Several factors affect the adsorption process, such as the molecular structure or nature of the sorbent, solubility of the solute, pH and temperature of the medium, and molecular diameter of the adsorbate (Foust et al., 1982). In studies of the area, the activated carbon adsorbent has been one of the most widely used in color removal and treatment of textile effluents. Furthermore, the development of low-cost alternative adsorbents has been the focus of many researches (Choi et al., 2015; Fernandez et al., 2015; Gonzalez et al., 2009; Kazmierczak-Razna et al., 2015; Khandelwal and Gaikwad, 2011; Saucier et al., 2015; Zhao et al., 2015).

In this way, bone char (BC) is a mixed adsorbent synthesized from the pyrolysis of bovine bone wastes and its adsorption behavior can be tailored for a specific pollutant. It is constituted by carbon and calcium phosphate, which is in the hydroxyapatite form (Medellin-Castillo et al., 2014; Zúñiga-Muro et al., 2017). Several studies have concluded that the dye adsorption properties of BC are attributed to their content of mineral components, especially, the hydroxyapatite content. Recent studies used BC to adsorb dyes from aqueous solution (Ip et al., 2009; Reynel-Avila et al., 2016). These authors suggested that chemisorption was the main operating mechanism. Authors claimed that sorption is based on electrostatic interactions. Therefore, according to Mendoza-Castillo et al. (2016) the production of low-cost BC for the treatment of industrial water polluted by dyes has increased its importance and relevance especially in developing countries.

The objectives of this study were to investigate the removal of Royal Blue Tiafix and Black Tiassolan dyes by BC, to identify the key factors controlling the batch adsorption process using a full factorial design, to optimize the adsorption conditions using 2^3 factorial

designs, and to evaluate suitable isotherm and kinetic models describing the adsorption process.

Experimental

Materials

BC supplied by Bonechar Carvão do Brasil Ltda, BR was used as adsorbent. The material when sieved according to methodology described by Allen (1981) had a mean particle diameter of 0.149 mm. Two different dyes with different colors both classified as "azo dyes" named Royal Blue Tiafix (AR.TF) and Black Tiassolan (P.TS) were gently donated from Aupicor Química Ltda, BR. When submitted to pH analysis they present pH equal to 5.1. Deionized water was used throughout for solution preparations. All reagents used were of analytical grade. Sodium hydroxide, potassium bromide (KBr), and hydrochloric acid were obtained from Aldrich and used as received.

Adsorbent characterization

Specific surface area, total volume of pores, pore diameter, and micropore volume of the activated carbon were performed at Central Analytics Multiuser Lab of IQ UFG, by nitrogen adsorption/desorption isotherms measurements at 77 K, using a Micromeritics ASAP, 2020 instrument. Before measurement, sample was pretreated for 24 h at 130°C to eliminate the superficially adsorbed water. Next, 0.250 g of carbon sample was submitted to a N_2 stream. The surface area was determined using the Langmuir equation.

Powder X-ray diffraction patterns were collected at Central Analytics Multiuser Lab of IQ UFG using a Shimadzu powder diffractometer with Cu–Kα (λ = 1.54 Å) radiation equipped with a graphite monochromator, operating at 40 kV and 30 mA in the 2Θ range of 10–80° at a scanning rate of 2° per minute.

A scanning electron microscope (SEM), Jeol, JSM-6610, equipped with EDS, Thermo Scientific NSS Spectral Imaging, of IF UFG, was used to determine the morphology of the sample. In this analysis, the adsorbent was metalized with aurum, by Shimadzu IC-Metalizer.

For chemical characterization, surface functional groups on the sample were studied by a Fourier transform infrared spectrometer (FT-IR). The FT-IR spectroscopic measurements were carried out using a Perkin Elmer 400 spectrophotometer at Central Analytics Multiuser Lab of IQ UFG. The BC was dried in a stove for 8 h at 100°C. Then, it was ground, mixed, and pressed with KBr in a proportion of 5% of carbon to make a small pellet of sample. The spectra were recorded in the range 400–4000 cm^{-1}, with eight scans for each reading, searching for a greater reliability.

Adsorption kinetics

The adsorption kinetics were carried out by 50 ml of a 200 mg l^{-1} of each dye solution with 50 mg of the BC. The dye solutions were stirred using an orbital shaker in a 125 ml Erlenmeyer flasks sealed with parafilm to avoid evaporation. The adsorption experiments were conducted at various time (from 0 to 1440 min) intervals at 25°C and 150 r min^{-1} in order to determine the adsorption equilibrium time. The solutions were filtered and then subjected to quantitative analyses. The concentrations of each solution collected at predetermined times were determined from the absorbance of the solution measured by

a spectrophotometer (Perkin Elmer Lambda 45 UV/VIS). The amount of dye adsorbed onto the BC surface was determined by the difference between the initial and remaining concentrations of each dye solution. The amount of adsorbed dye at time t, q_t (mg g^{-1}) was calculated according to equation (1)

$$q_t = \frac{V\ (C_0 - C_t)}{m} \tag{1}$$

whereas q is the amount of the dye adsorbed on the solid phase (mg g^{-1}) at time t, C_t is the dye concentrations in bulk of solution at time t (mg l^{-1}), V is the volume of dye solution (l), and "m" is the weight of adsorbent (g).

Experimental design

The factorial design chosen to be applied in this work was a 2^3 central composite, which indicates a factorial experiment with three control factors, each tested in two levels (encoded by -1 and 1). The experimental design matrix was generated using the software Statistica™. The high and low levels defined for the 2^3 factorial designs can be consulted in supplementary materials.

Taking into account the statistical analyzes to be carried out, it was defined the control factors, that is those which are deliberately altered in the experiments: agitation (A), temperature (T), and pH. As a response variable, that is the one that undergoes the effects in the experiments when stimuli are introduced purposively in the control factors, the adsorption capacity (q_e) was adopted.

For the experiments, solutions were prepared from a 200 mg l^{-1} stock solution for each dye. The pH of the solutions was carefully adjusted with adding a small amount of dilute HCl or NaOH solution using a pH meter (Hanna Instruments HI 8314). Tests were performed in 125 ml Erlenmeyer flasks containing 40 ml of the solution with adjusted pH and 40 mg of BC. Before the addition of adsorbent an aliquot of each point was taken for later absorbance reading. The test duration was 10 h under agitation in an orbital shaker (Tecnal, TE-4200). At the end of the test, aliquots were removed, filtered, and stored. A standard curve was developed at λ_{max} 591 and 572 nm for AR.TF and P.TS, respectively, through the measurement of each dye solution absorbance by a UV/Vis Spectrophotometer. The absorbance was read from the pretest and posttest aliquots, using the Perkin Elmer Lambda 45 UV/VIS Spectrometer. The results obtained were used to calculate the adsorption capacity (q_e) according to equation (2)

$$q_e = \frac{V\ (C_0 - C_e)}{m} \tag{2}$$

where q_e is the dye equilibrium concentration in the solid phase (mg g^{-1}) and C_e (mg l^{-1}) is the dye equilibrium concentration in the liquid phase.

Adsorption equilibrium

The procedures for the equilibrium experiments were basically identical to those of kinetics tests. The aqueous samples with different concentrations (60, 80, 100, 160, 200, 260, 300,

400, 500, and 600 mg l^{-1}) were taken after 10 h of stirring with 40 mg of adsorbent and the concentrations of each dye were similarly measured. The amount of adsorption at equilibrium, q_e (mg g^{-1}), was calculated by equation (2). The equilibrium data were fitted to Langmuir and Freundlich models, with the purpose of obtaining parameters such as the maximum adsorption capacity (q_{max}).

Results and discussions

Characterization

The N_2 adsorption/desorption isotherms provide a textural characterization of the BC adsorbent. The parameters obtained were the specific surface area, total pore volume, micropore volume, and average pore diameter. Figure 1 shows the N_2 adsorption and desorption Langmuir isotherm for the BC. According to IUPAC classification, the observed isotherm profile indicated a Type IV isotherm which is typical for mesoporous materials. Furthermore, the isotherm also has a Type H3 hysteresis which is associated with the predominance of pores in parallel plates form. From pore size distribution, it can be seen that BC surface is essentially mesoporous, since it has high incidence of pore diameters between 20 and 100 Å (Bedin et al., 2017; Poinern et al., 2011).

Table 1 presents the textural properties of the adsorbent. The average pore diameter of BC was 99.5 Å. The result of the application of the BJH method showed a larger amount of mesopore volume (20 Å < pore diameter < 500 Å), representing approximately 98% of the total pore volume.

The surface morphology of the BC adsorbent is shown in Figure 2. The BC presents an irregular and disorganized mesoporous structure without very well-defined pores. By increasing 5000 times (Figure 2(c)) it is possible to observe the pores where the adsorption

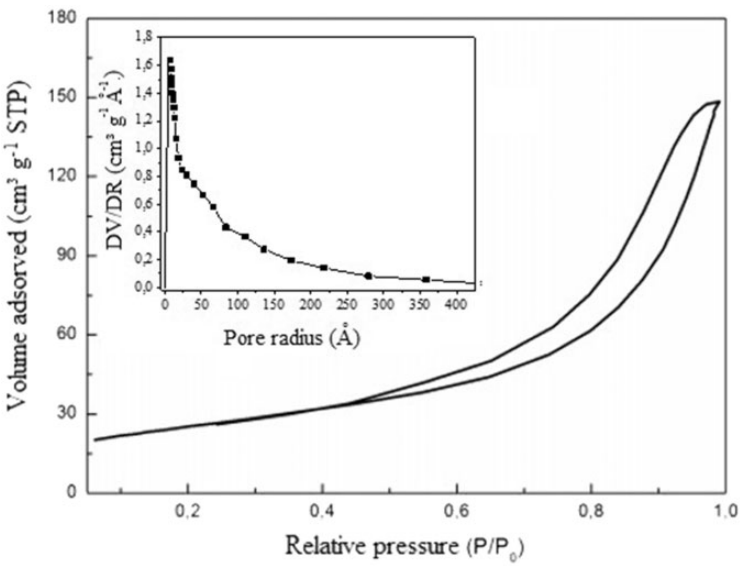

Figure 1. N_2 adsorption/desorption isotherm at 77 K.

Table 1. Morphological characteristics of BC adsorbent obtained by N_2 physisorption.

Specific surface area ($m^2\ g^{-1}$)	Mesopore area ($m^2\ g^{-1}$)	Pore diameter (Å)	Total pore volume ($cm^3\ g^{-1}$)	Mesopore volume ($cm^3\ g^{-1}$)	Micropore volume ($cm^3\ g^{-1}$)	Type of adsorbent
123.1	111.3	99.5	0.22	0.215	0.005	Mesoporous

BC: bone char.

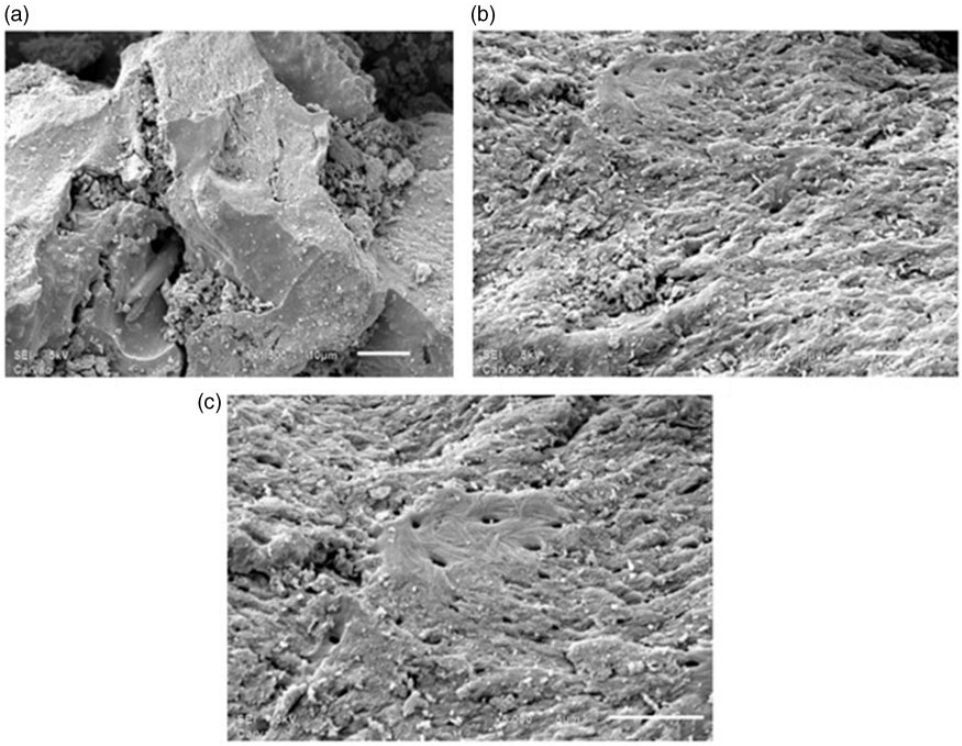

Figure 2. SEM images of BC particles (a) increased 1500 times, (b) increased 3000 times, and (c) increased 5000 times.

process takes place. This result is in agreement with those observed by previous works (Medellin-Castillo et al., 2014; Winter et al., 2016).

Figure 3 shows the X-ray diffraction profile of BC. The BC is a mixed adsorbent in which the carbon is distributed along a porous structure of hydroxyapatite (Ca10(PO4)6(OH)2). The crystalline species of BC was identified by comparing the characteristic peaks shown using the database of the diffractometer available in the *Journal of Crystallographic Powder Diffraction*. The peaks can be observed at 26°, 32°, 40°, 46.8°, and 49.6°, which correspond to (002), (211), (310), (222), and (213) Miller planes. According to Medellin-Castillo et al. (2014) and Tang et al. (2010) these peaks confirm the calcium hydroxyapatite structure of BC. Furthermore, the crystallite size values were calculated by the Scherrer's equation, taking the most intense peak and the Gaussian model. The crystallite size of BC is 4.97 nm.

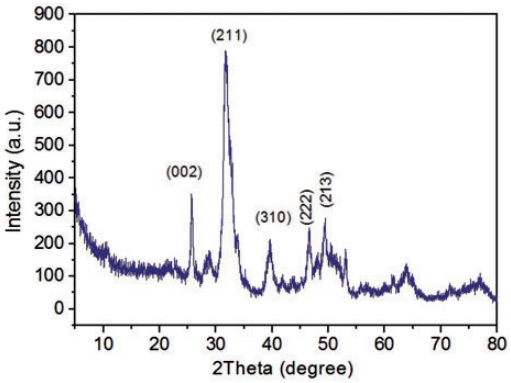

Figure 3. XRD spectrum of BC adsorbent.

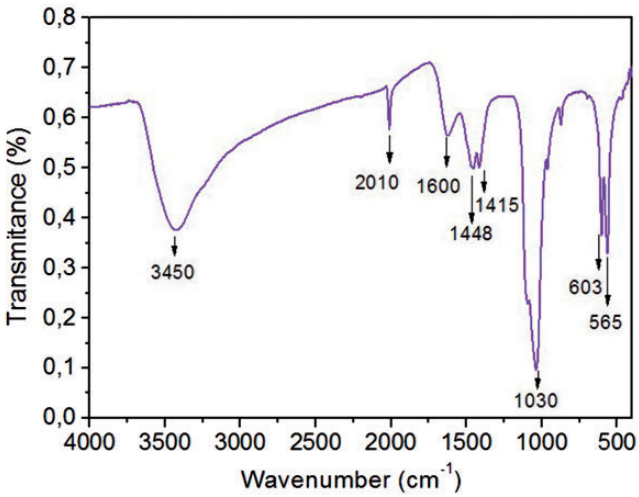

Figure 4. FT-IR spectrum of BC adsorbent.

The FT-IR spectrum was conducted to determine the functional groups of the material. The FT-IR analysis of BC was presented in Figure 4 and it can be noted that the results agree with information obtained by XRD patterns, where the characteristic peaks of hydroxyapatite are evident. The OH stretching vibration appearing at 3300–3450 cm^{-1} was attributed to the presence of phenols, alcohols, and carboxylic group. Also, the fact that this band is wide may be due to the presence of adsorbed water (Patel et al., 2015). The C = O and C = C stretching vibrations of protein and collagen on bovine bone are present in the 1500–1600 cm^{-1} range (Bedin et al., 2017). The bands at 1448–1415 cm^{-1} are due to the C–O stretching and has been assigned to CO_3^{-2} group, while the signals at 565, 603, 1030, and 2010 cm^{-1} are characteristics of stretching and bending vibrations of PO_4^{3-} groups (Ahmed et al., 2015; Delgadillo-Velosco et al., 2017; Patel et al., 2015; Tovar-Gomez et al., 2013).

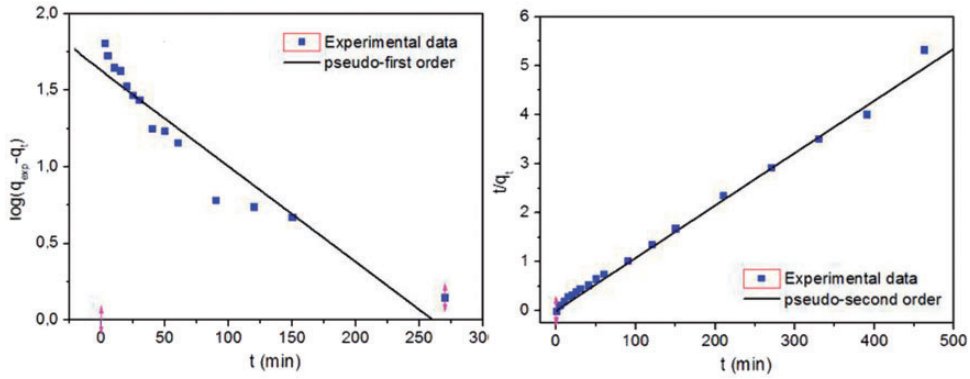

Figure 5. Linear adjustment for models of pseudo-first and pseudo-second order for AR.TF dye.

Adsorption kinetics

For the study of kinetic adsorption, it is necessary to know the time of adsorption to reach the equilibrium. It can be observed that AR.TF dye shows fast kinetics, reaching equilibrium after 1 h and 30 min of contact time. As for the P.TS dye, it took 4 h and 50 min of testing until this equilibrium was finally achieved.

In this paper, three kinetic models were used to mathematically describe the adsorption constants. The linearized forms of the pseudo-first-order (Lagergren, 1898) and pseudo-second-order (Blanchard et al., 1984) models are described in equations (3) and (4), respectively. The pseudo-first-order equation is based on the assumption that the adsorption is preceded by physical diffusion while the pseudo-second-order equation might predict the whole adsorption behavior, in which the chemisorption would be the rate-limiting step (Purkait et al., 2005)

$$\log(q_e - q_t) = \log q_e - \frac{k_1}{2,303} t \tag{3}$$

$$\frac{t}{q_t} = \frac{1}{k_2 q_e^2} + \frac{1}{q_e} \tag{4}$$

where k_1 (min^{-1}) and k_2 ($\text{g mg}^{-1}\ \text{min}^{-1}$) are the rate constants of the pseudo-first-order and pseudo-second-order models, respectively and q_e and q_t are the AR.TF or P.TS dyes uptake per mass of BC at equilibrium and at any time t (min), respectively. The best fitted model was considered based on the regression coefficient (R^2) and the experimental q_e value obtained.

The kinetics adsorption studies are shown in Figures 5 and 6. The parameters of kinetics equations are presented in Table 2. As shown in Table 2 the kinetics of AR.TF and P.TS dyes removal by the use of BC followed pseudo-second-order equation ($R^2 > 0.99$) indicating the chemical nature of the adsorption process. It can also be noticed that for the pseudo-second order the calculated adsorption capacity, q_{cal}, values obtained from the model approximate with those values obtained from experiments, q_e. The error percentages

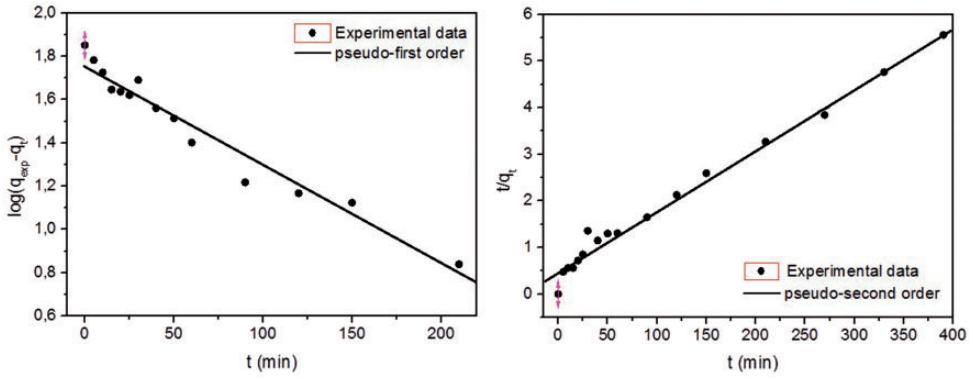

Figure 6. Linear adjustment for models of pseudo-first order and pseudo-second order for P.TS dye.

Table 2. Pseudo-first- and second-order parameters.

Model	Parameters	Dye AR.TF	P.TS
Pseudo-first order	q_{exp} (mg g^{-1})	93.8	71.1
	k_1 (min^{-1})	0.00639	0.01353
	q_{calc} (mg g^{-1})	46.6	52.3
	R^2	0.82	0.93
Pseudo-second order	q_{exp} (mg g^{-1})	93.8	71.1
	k_2 (g mg^{-1} min^{-1})	0.00117	0.00037
	q_{cal} (mg g^{-1})	94.3	76.3
	R^2	0.99	0.99

AR.TF: Royal Blue Tiafix; P.TS: Black Tiassolan.

between the experimental and calculated adsorption capacities for the AR.TF and P. dyes were 0.5 and 6.8%, respectively.

Factorial design

AR.TF dye. The results of the adsorption capacity (q_e) obtained for the AR.TF dye were analyzed statistically by the experimental design, using the Statistica™ software. In the experimental design in question was adopted at the 90% significance level, that is the parameters were considered significant with p values < 0.1. Table 3 shows that the greatest value to the adsorption capacity (q_e), 97.4 mg g^{-1}, was acquired in Experiment 8 at 150 r min^{-1} agitation, 35°C temperature, and pH 6. Experiment 12 showed 92.6 mg g^{-1} at the rotation 110 r min^{-1}, 38.4°C temperature, and pH 5. At last, in Experiment 7 the adsorption capacity was 88.5 mg g^{-1} at 150 r min^{-1} rotation, 35°C, and pH 4. The best results of q_e that appeared in the design were found in the three previously mentioned experiments. Evaluating the factors that generated said responses it is noticeable that they occurred at higher temperatures. However, considering Experiments 1 and 5 we can see the lowest values for the adsorption capacity, respectively, 40.4 and 41.5 mg g^{-1}. These responses have the lowest temperature levels (25°C) in common. Therefore, it is possible to infer

Table 3. Matrix factorial design with the results of the adsorption capacity for the dye AR.TF.

Experiment	Agitation (r min^{-1})	Temperature (°C)	pH	q_e (mg g^{-1})
1	(−1) 70	(−1) 25	(−1) 4	47.9
2	(−1) 70	(−1) 25	(1) 6	51.1
3	(−1) 70	(1) 35	(−1) 4	61.1
4	(−1) 70	(1) 35	(1) 6	64.4
5	(1) 150	(−1) 25	(−1) 4	41.5
6	(1) 150	(−1) 25	(1) 6	45.7
7	(1) 150	(1) 35	(−1) 4	88.5
8	(1) 150	(1) 35	(1) 6	94.5
9	(−1.68) 42.7	(0) 30	(0) 5	52.5
10	(1.68) 177.3	(0) 30	(0) 5	64.8
11	(0) 110	(−1.68) 21.6	(0) 5	47.0
12	(0) 110	(1.68) 38.4	(0) 5	92.6
13	(0) 110	(0) 30	(−1.68) 3.32	59.7
14	(0) 110	(0) 30	(1.68) 6.68	57.3
15	(0) 110	(0) 30	(0) 5	49.9
16	(0) 110	(0) 30	(0) 5	50.5
17	(0) 110	(0) 30	(0) 5	50.9

AR.TF: Royal Blue Tiafix.

Table 4. Multiple regression with the significant variables, their factors and interactions, and significance levels for the adsorption of the dye AR.TF.

Factors and interactions	Regression coefficient	Level of significance (p)
Independent term	50.50987	0.000000
Agitation (L)	4.86833	0.00048
Agitation (Q)	2.64140	0.007373
Temperature (L)	14.57801	0.000000
Temperature (Q)	6.58352	0.000008
pH (Q)	2.58836	0.008259
Agitation*temperature	8.67500	0.000003
$R^2 = 0.984$		

AR.TF: Royal Blue Tiafix.

that the adsorption of the dye AR.TF by BC occurs more effectively at temperatures higher than 35°C.

Table 4 shows the analysis of all the main effects and interactions of multiple regression obtained from the results of Table 3 for the adsorption of the dye AR.TF.

After adjusting the model with only the significant variables, we obtain equation (5). It is valid to highlight the good linear correlation coefficient (R^2) achieved by the studied model (0.984) which indicates a good fit of the data to model in question. Also, Figure 7 shows the response surface and the contour based on equation (5)

$$[Adsorption\ \ Capacity] = 50.50 + 4.86 \cdot A + 2.64 \cdot A^2 + 14.57 \cdot T + 6.58 \cdot T^2 + 2.58 \cdot pH^2 + 8.67 \cdot A{*}T \quad (5)$$

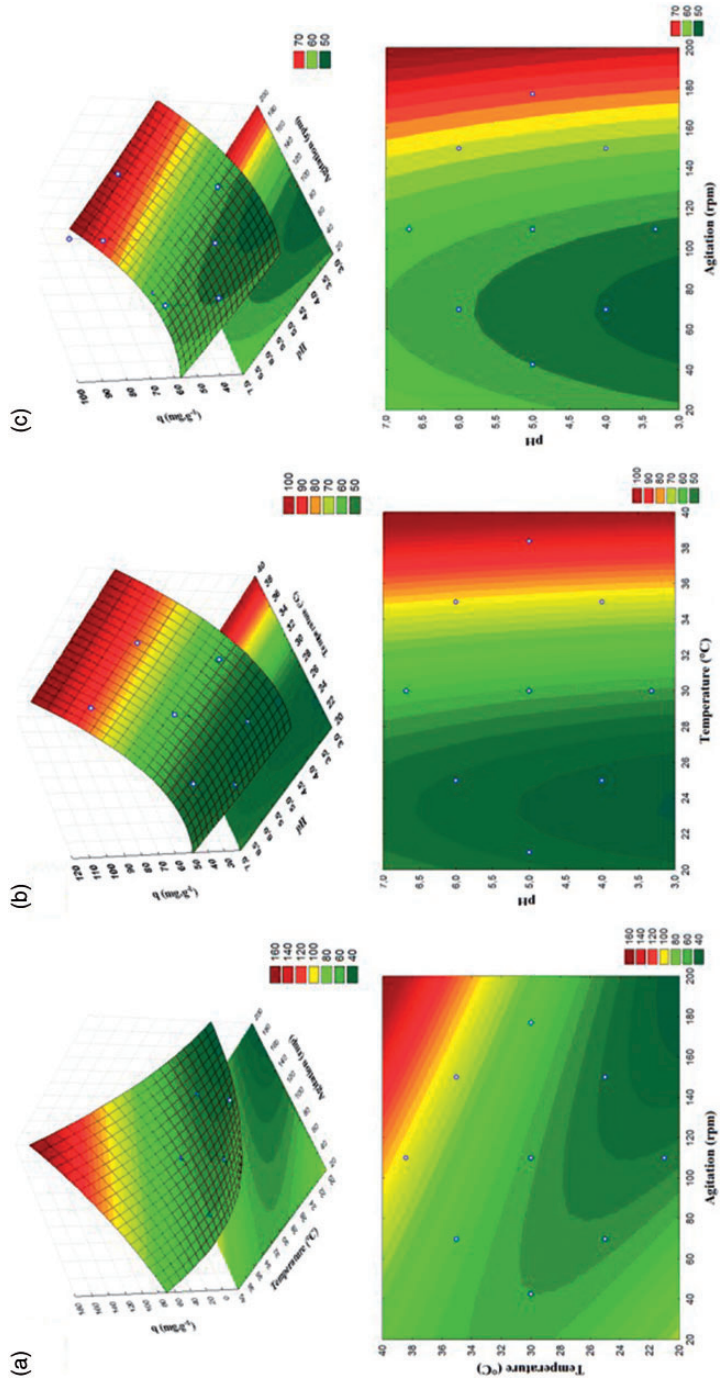

Figure 7. Response surface and contour of AR.TF dye adsorption considering (a) agitation versus temperature, (b) pH versus temperature, and (c) agitation versus pH.

In Figure 7(a) it can be noted by the response and contour surface that in higher temperatures and agitation is obtained the best adsorption capacity. This statement confirms the data presented in Table 3, where in Experiment 8 (temperature 35°C and stirring 150 r min^{-1}) was presented the highest value of q_e (94.5 mg g^{-1}) in this study for dye AR. TF.

Considering the pH versus temperature data, Figure 7(b) reinforces that at temperatures around 38°C there is an increase in the adsorption capacity. Whereas Experiment 12, shown in Table 3, it is observed that at a temperature of 38.7°C was obtained the second highest value for q_e of 92.6 mg g^{-1}. Also, it can be noted that the pH does not influence directly in the adsorption process which may allow a more extensive pH range for studying the adsorption of the AR.TF dye on BC.

According to Figure 7(c), which makes up the response surface and the contour considering agitation versus pH, it follows that on higher agitation values the adsorption capacity is better represented. Analyzing the pH in this situation there has been a slight change considered positive for higher values of pH.

The rate of adsorption of AR.TF in aqueous solution increases with the temperature of the reaction medium, in accordance with the study of Aboua et al. (2015) and Karim et al. (2006). According to these authors, the increase in adsorption with temperature may be due either to the chemical interaction intensification between the ions of the adsorbent and the surface groups of the BC or to an increase of the intraparticle diffusion rate of the ions of the adsorbate in the pores at elevated temperatures.

Cestari et al. (2004) investigated the adsorption of a yellow dye on chitosan beads and the influence of its chemical structures and temperature. It was observed that adsorption of the dye increases with increasing temperature. The authors believe the behavior is related to the intrinsic characteristics of the yellow dye, which present a relatively linear and small carbonic chain, which can spread out into the inner part of the microbeads with gradually increasing temperature.

P.TS dye. In an analogous way to what was done for the AR.TF dye, the results of adsorption capacity (q_e) obtained in P.TS dye adsorption study were also analyzed statistically by the experimental design using the Statistica™ software. The 90% level of significance was kept, considering the significant parameters with p values < 0.1. Through examination of Table 5 it was noted that in Experiment 10 (177.3 r min^{-1}, 30°C, and pH 5) that presents the highest value for the adsorption capacity ($q_e = 36.3$ mg g^{-1}) for the P. TS dye. However, Experiment 5 had 31.7 mg g^{-1}, with rotation 150 r min^{-1}, temperature 25°C, and pH 4. In Experiment 11 the adsorption capacity was 28.5 mg g^{-1} at 110 r min^{-1}, 21.6°C, and pH 5. Finally, Experiments 1 and 9 also found considerable levels of adsorption capacity for the P.TS dye. In these cited experiments, the best q_e results are seen in greater agitation levels and lower pH. Thus, through this information it is possible to assume that the adsorption of the dye P.TS by BC is more effective at lower pH and higher agitation.

The multiple regression analysis of all the main effects and the interactions obtained from the results of Table 5 for the adsorption of the dye P.TS are shown in Table 6.

Adjusting the model taking into account now only significant variables, we obtain equation (6). The linear correlation coefficient (R^2) obtained for the model was 0.98

Table 5. Matrix factorial design with the results of the adsorption capacity for the dye P.TS.

Experiment	Agitation (r min^{-1})	Temperature (°C)	pH	q_e (mg g^{-1})
1	(−1) 70	(−1) 25	(−1) 4	27.7
2	(−1) 70	(−1) 25	(1) 6	17.5
3	(−1) 70	(1) 35	(−1) 4	19.8
4	(−1) 70	(1) 35	(1) 6	18.5
5	(1) 150	(−1) 25	(−1) 4	31.7
6	(1) 150	(−1) 25	(1) 6	19.2
7	(1) 150	(1) 35	(−1) 4	23.7
8	(1) 150	(1) 35	(1) 6	21.3
9	(−1.68) 42.7	(0) 30	(0) 5	26.5
10	(1.68) 177.3	(0) 30	(0) 5	36.3
11	(0) 110	(−1.68) 21.6	(0) 5	28.5
12	(0) 110	(1.68) 38.4	(0) 5	21.3
13	(0) 110	(0) 30	(−1.68) 3.32	22.5
14	(0) 110	(0) 30	(1.68) 6.68	6.86
15	(0) 110	(0) 30	(0) 5	20.4
16	(0) 110	(0) 30	(0) 5	19.7
17	(0) 110	(0) 30	(0) 5	20.9

P.TS: Black Tiassolan.

Table 6. Multiple regression with the significant variables, their factors and interactions, and significance levels for the adsorption of the dye P.TS.

Factors and interactions	Regression coefficient	Level of significance (p)
Independent Term	20.38482	0.000000
Agitation (L)	3.41535	0.000073
Agitation (Q)	1.96220	0.000002
Temperature (L)	−1.89421	0.000096
Temperature (Q)	1.43721	0.001345
pH (L)	−3.65089	0.000000
pH (Q)	−2.37409	0.000035
Temperature*pH	2.25500	0.000192
$R^2 = 0.98$		

P.TS: Black Tiassolan.

indicating a good fit of the data. Figure 8 shows the response surface and the contour based on equation (6)

$$[Adsorption\ \ Capacity] = 20.38 + 3.41 \cdot A + 1.96 \cdot A^2 - 1.89 \cdot T + 1.43 \cdot T^2 - 3.65 \cdot \mathrm{pH} - 2.37 \cdot pH^2 + 2.25 \cdot T{*}pH \quad (6)$$

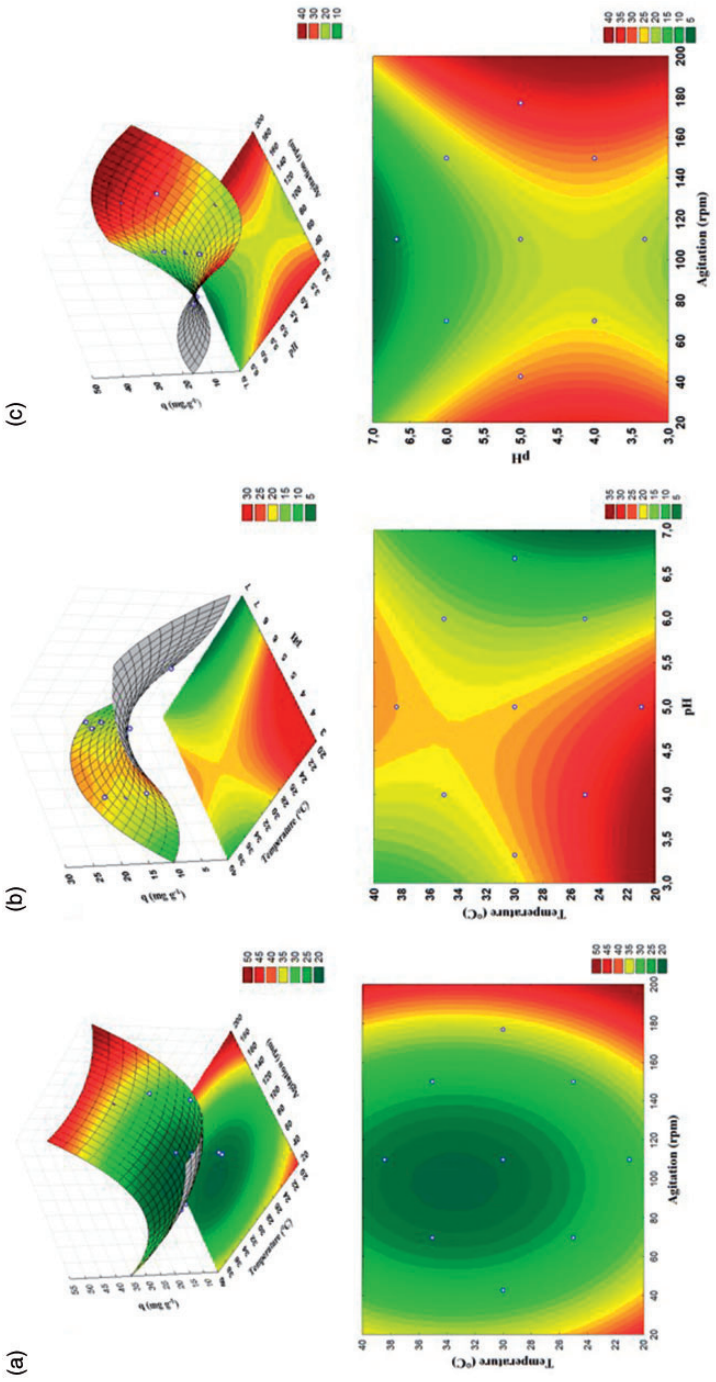

Figure 8. Response surface and contour of PTS dye adsorption considering (a) agitation versus temperature, (b) pH versus temperature, and (c) agitation versus pH.

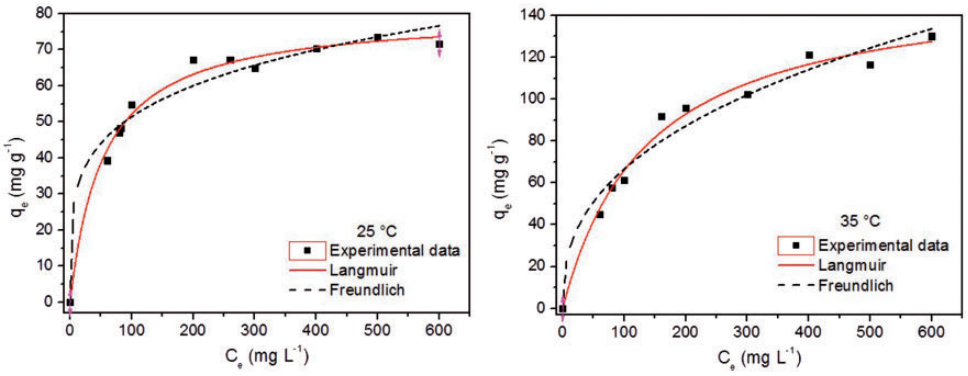

Figure 9. Adsorption isotherm plots of the Langmuir and Freundlich models for AR.TF adsorption on BC 25 and 35°C.

In Figure 8(a) it is remarkable that the adsorption of the dye P.TS gave higher responses at lower temperatures when considering the interaction of temperature and agitation. For example, in Experiments 1 and 11 it was obtained 27.7 and 28.5 mg g^{-1} for adsorption capacity. By analysis of the response and the level curved surface represented by Figure 8(b), it can be observed that at lower pH values, the adsorption capacity is increased. With the pH value at 4 in Experiment 5 was observed $q_e = 31.7$ mg g^{-1}, which is the highest given in this study for the dye P.TS. The behavior seen in Figure 8(c) is similar to those cited in Figure 8 (b), which reinforces the suggestion at pH's lower adsorption of the dye P.TS occurs more effectively. Overall, when compared to studies of adsorption of AR.TF and P.TS dyes it is important to note that for the first adsorption with BC was better. This fact can be confirmed by making a comparison of the data presented in Tables 3 and 5.

Hence, it can be concluded that the adsorption of P.TS onto BC is higher at low pH due to electrostatic attraction. Similar behavior was observed for adsorptions of azo disperse dye when increasing the pH from 1.0 to 7.0, resulting in a decrease of removal efficiency by Tezcan Un et al. (2015) and Wang et al. (2012).

Bingol et al. (2010) studied the Brilliant Yellow dye adsorption onto sepiolite using a full factorial design. In their work, between the parameters evaluated (temperature, initial pH of the solution, and ionic strength of the dispersion), the initial pH also exerted the greatest influence on the amounts of dye adsorbed q_e.

Adsorption equilibrium

The adsorption equilibrium study was conducted for AR.TF and P.TS considering the best conditions obtained in the experimental design for each dye. The adsorption equilibrium was obtained by plotting the experimental amount of dye adsorbed, q_e (mg g^{-1}), against each dye concentration, C_e (mg l^{-1}), under equilibrium conditions (Figures 9 and 10). To identify the mechanisms of adsorption process, two types of isotherm model were tested for fitting the adsorption data, namely the Langmuir isotherm (Langmuir, 1918) and the Freundlich isotherm (Freundlich, 1906). The nonlinear regression analysis was carried out to examine the parameters and the correlation coefficient (R^2).

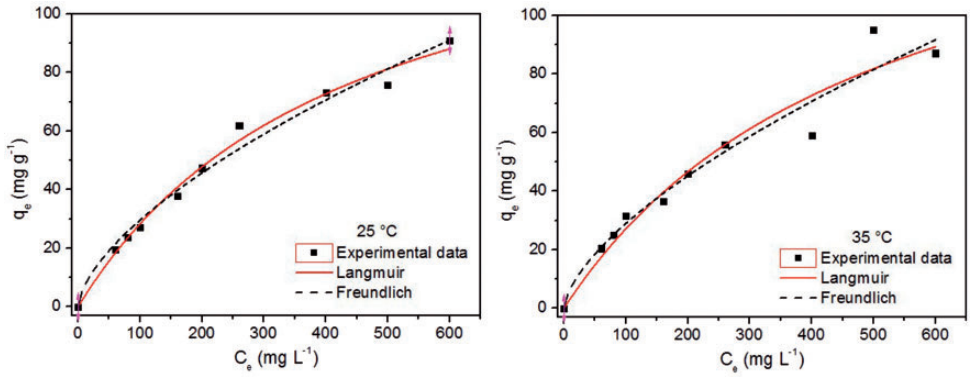

Figure 10. Adsorption isotherm plots of the Langmuir and Freundlich models for P.TS adsorption on BC at 25 and 35°C.

Langmuir isotherm model can be described as follows

$$q_e = \frac{q_{max}.K_L.C_e}{1 + K_L.C_e} \tag{7}$$

where K_L is the Langmuir constant related to the affinity of the dye molecules to the adsorbent (l mg^{-1}) and q_{max} is the maximum monolayer adsorption capacity (mg g^{-1}).

The essential characteristics of Langmuir equation can be expressed in terms of dimensionless separation factor, R_L defined as

$$R_L = \frac{1}{1 + K_L C_0} \tag{8}$$

where C_0 is the initial concentration of AR.TS or P.TS dyes, the R_L value implies whether the adsorption is unfavorable: $R_L > 1$; linear: $R_L = 1$; favorable: $0 < R_L < 1$ and irreversible: $R_L = 0$.

Freundlich isotherm model can be described as follows

$$q_e = K_F.C_e^{\frac{1}{n}} \tag{9}$$

where K_F ((mg g^{-1}) (l mg^{-1})$^{1/n}$) is the Freundlich isotherm constant and $1/n$ is the value that is used to indicate the heterogeneity of the adsorbent's surface. As $1/n$ is closer to zero, the surface becomes more heterogeneous. Tables 7 and 8 summarize the calculated parameters of the two isotherm models for AR.TS an P.TS dyes, respectively.

When comparing the R^2 values of both dyes studied, presented in Tables 7 and 8, it is possible to infer that experimental data best fit with the Freundlich model at different temperatures, except for the P.TS at temperature of 25°C, which presents a best fit for Langmuir model (R^2 0.9888). While the increase in temperature favors the adjustment to the Langmuir model for P.TS, for AR.TS this increase causes the Freundlich model best fit.

The Freundlich isotherm is used for nonideal adsorption which involves systems with heterogeneous surface energy. It assumes that the adsorption occurs at sites of different

Table 7. Parameters of the Langmuir and Freundlich isotherm models for AR.TF adsorption on BC at different temperatures.

		Temperature (°C)	
Model	Parameter	25	35
Langmuir	q_{max} (mg g^{-1})	73.91	129.21
	K_L	0.0549	0.0280
	R_L	0.2241	0.3581
	R^2	0.9868	0.9695
Freundlich	K_F	26.79	25.14
	$1/n$	0.1639	0.2638
	R^2	0.9935	0.9909

AR.TF: Royal Blue Tiafix; BC: bone char.

Table 8. Parameters of the Langmuir and Freundlich isotherm models for P.TS adsorption on BC at different temperatures.

		Temperature (°C)	
Model	Parameter	25	35
Langmuir	q_{max} (mg g^{-1})	152.15	162.24
	K_L	0.0023	0.0020
	R_L	0.8792	0.8928
	R^2	0.9888	0.9707
Freundlich	K_F	1.65	1.50
	$1/n$	0.6264	0.6427
	R^2	0.9821	0.9783

BC: bone char; P.TS: Black Tiassolan.

energies by physisorption. However, in the Langmuir model adjustments shown in Tables 7 and 8, considerable R^2 values were also obtained, which possibly indicate the tendency of the adsorption process studied to coexist with monolayer and multilayer adsorption, respectively, chemical and physical adsorption. The Langmuir isotherm assumes that the adsorption occurs in a monolayer, in which the molecules are adsorbed and adhere to the surface of the adsorbent in well-defined and localized sites (chemisorption).

A possible explanation for the great fit of the Freundlich model for BC is that this adsorbent is composed primarily of carbon and calcium phosphate in the form of hydroxyapatite, being randomly distributed over the surface of the BC (Moreno et al., 2010).

An analysis of parameter $1/n$ from Freundlich model shows that for both dyes the adsorption is a favorable process, once all values obtained were less than 1. The same can be observed by the R_L parameter form Langmuir model which presents values less than 1 for all dyes in different temperatures. Also by the analysis of q_{max} from Langmuir model it is possible to observe for both dyes the increase in temperature caused an increase in the adsorption capacity (73.91–129.21 mg g^{-1} for AR.TS and 152.15–162.24 mg g^{-1}

Table 9. Overview of maximum adsorption capacity of different dyes using bone char as adsorbent.

Dye	Maximum adsorption (mg g^{-1})	Reference
Royal Blue Tiafix[a]	129.2	In this work
Black Tiassolan[a]	162.2	
Reactive Black 5	160.0	Ip et al. (2009)
Acid Blue 74	45.8	Reynel-Avila et al. (2016)
Reactive Blue 4	89.1	
Methylene Blue	5.0	Ghanizadeh and Asgari (2011)
Tectilon Blue 4R-01	476	Walker and Weatherley (2001)
Tectilon Red 2B	508	
Tectilon Orange 3G	477	

[a]At 35°C.

for P.TS). Table 9 shows some studies in which BC was used for the adsorption of different dyes.

Conclusions

This study evaluated the potential use of BC as adsorbent for removal of the Royal Blue Tiafix (AR.TF) and P.TS dyes from aqueous solutions. Based on the kinetics analyses performed in this paper, it appears that the uptake of both dyes on BC adsorbent is by chemisorption control. The factorial design identified the factors that most affected the adsorption process. For the AR.TF dye, the temperature had the greater influence. The pH showed to be active in the adsorption of the P.TS dye. Adsorption equilibrium data follow Freundlich isotherm equation for AT.TS dye while the data were fitted using Langmuir and Freundlich isotherm equations for the P.TS dye. The results obtained during this work showed that the BC presented to be a good adsorbent for the AR.TF and P.TS dyes. However, for further work the optimization of the factorial design conditions could be done to increase the adsorption capacity of the adsorbent.

Acknowledgment

The authors are grateful to Multiuser Analysis Center from IQ-UFG for the technical-scientific support and to Bonechar Carvão do Brasil Ltda for the activated carbon gently donated.

Declaration of Conflicting Interests

The author(s) declared no potential conflicts of interest with respect to the research, authorship, and/or publication of this article.

Funding

The author(s) disclosed receipt of the following financial support for the research, authorship, and/or publication of this article: The authors are grateful to CAPES (Coordination for the Improvement of Higher Education Personnel) for financial support.

ORCID iD

Fernanda F Freitas http://orcid.org/0000-0002-1670-5094

References

Aboua KN, Yobouet YA, Yao KB, et al. (2015) Investigation of dye adsorption onto activated carbon from the shells of Macoré fruit. *Journal of Environmental Management* 156: 10–14.

Ahmed YMZ, El-Sheikh SM and Zaki ZI (2015) Changes in hydroxyapatite powder properties via heat treatment. *Bulletin of Materials Science* 38: 1807–1819.

Allen T (1981) *Particle size measurement*. 3 rd ed., Chapman and Hall, London.

Bedin KC, Azevedo SP, Leandro PKT, et al. (2017) Bone char prepared by CO_2 atmosphere: Preparation optimization and adsorption studies of Remazol Brilliant Blue R. *Journal of Cleaner Production* 161: 288–298

Belhouchat N, Zaghouane-Boudiaf H and Viseras C (2017) Removal of anionic and cationic dyes from aqueous solution with activated organo-bentonite/sodium alginate encapsulated beads. *Applied Clay Science* 135: 9–15.

Bingol D, Tekin N and Alkan M (2010) Brilliant Yellow dye adsorption onto sepiolite using a full factorial design. *Applied Clay Science* 50(3): 315–321.

Blanchard G, Maunaye M and Martin G (1984) Removal of heavy-metals from waters by means of natural zeolites. *Water Research* 18(12): 1501–1507.

Cestari AR, Vieira EFS, Dos Santos AGP, et al. (2004) Adsorption of anionic dyes on chitosan beads. 1. The influence of the chemical structures of dyes and temperature on the adsorption kinetics. *Journal of Colloid and Interface Science* 280(2): 380–386.

Cheng Z, Zhang L, Guo X, et al. (2015) Removal of Lissamine rhodamine B and acid orange 10 from aqueous solution using activated carbon/surfactant: Process optimization, kinetics and equilibrium. *Journal of the Taiwan Institute of Chemical Engineers* 47: 149–159.

Choi GG, Oh S, Lee S, et al. (2015) Production of bio-based phenolic resin and activated carbon from bio-oil and biochar derived from fast pyrolysis of palm kernel shells. *Bioresource Technology* 178: 99–107.

Delgadillo-Velasco L, Hernández-Montoya V, Cervantes FJ, et al. (2017) Bone char with antibacterial properties for fluoride removal: Preparation, characterization and water treatment. *Journal of Environmental Management 201:* 277–285.

Fernandez ME, Ledesma B, Román S, et al. (2015) Development and characterization of activated hydrochars from orange peels as potential adsorbents for emerging organic contaminants. *Bioresource Technology* 183: 221–228.

Foust AS, Wenzel LA and Clump CW (1982) *Principles of Unit Operations*. New York: Wiley.

Freundlich H (1906) *Über die Adsorption in Lösungen*: *Zeitschrift für Physikalische Chemie*, Leipzig, 57A: 385-470.

Ghanizadeh G and Asgari G (2011) Adsorption kinetics and isotherm of methylene blue and its removal from aqueous solution using bone charcoal. *Reaction Kinetics, Mechanisms and Catalysis* 102(1): 127–142.

Gonzalez JF, Roman S, Encinar JM, et al. (2009) Pyrolysis of various biomass residues and char utilization for the production of activated carbons. *Journal of Analytical and Applied Pyrolysis* 85: 134–141.

Ip AWM, Barford JP and McKay G (2009) Reactive Black dye adsorption/desorption onto different adsorbents: Effect of salt, surface chemistry, pore size and surface area. *Journal of Colloid and Interface Science* 337(1): 32–38.

Islam MM, Mahmud K, Faruk O, et al. (2011) Textile dyeing industries in Bangladesh for sustainable development. *International Journal of Environmental Science and Development* 2(6): 428–436.

Karim MM, Das AK and Lee SH (2006) Treatment of colored effluent of the textile industry in Bangladesh using zinc chloride treated indigenous activated carbons. *Analytica Chimica Acta* 576(1): 37–42.

Karthik T and Rathinamoorthy R (2015) Recycling and reuse of textile effluent sludge. In: S MuthuS (ed) *Environmental Implications of Recycling and Recycled Products*. Singapore: Springer Singapore, pp.213–258.

Kazmierczak-Razna J, Gralak-Podemska B, Nowicki P, et al. (2015) The use of microwave radiation for obtaining activated carbons from sawdust and their potential application in removal of NO_2 and H_2S. *Chemical Engineering Journal* 269: 352–358.

Khandelwal SK and Gaikwad RW (2011) Removal of dyes from dye effluent using sugarcane bagasse ash as an adsorbent. *International Journal of Chemical Engineering and Applications* 2(3): 309–317.

Lagergren S (1898) On the theory of so-called adsorption dissolved substances. *Handlingar Band* 24: 1–39.

Langmuir I (1918) The adsorption of gases on plane surfaces of glass, mica and platinum. *Journal of the American Chemical Society* 40(9): 1361–1403.

Luo P, Zhao Y, Zhang B, et al. (2010) Study on the adsorption of Neutral Red from aqueous solution onto halloysite nanotubes. *Water Research* 44(5): 1489–1497.

Marrakchi F, Ahmed MJ, Khanday WA, et al. (2017) Mesoporous carbonaceous material from fish scales as low-cost adsorbent for reactive orange 16 adsorption. *Journal of the Taiwan Institute of Chemical Engineers* 71: 47–54.

Medellin-Castillo NA, Leyva-Ramos R, Padilla-Ortega E, et al. (2014) Adsorption capacity of bone char for removing fluoride from water solution. Role of hydroxyapatite content, adsorption mechanism and competing anions. *Journal of Industrial and Engineering Chemistry* 20(6): 4014–4021.

Mendoza-Castillo DI, Reynel-Ávila HE, Bonilla-Petriciolet A, et al. (2016) Synthesis of denim waste-based adsorbents and their application in water de fl uoridation. *Journal of Molecular Liquids* 221: 469–478.

Moreno JC, Gómez R and Giraldo L (2010) Removal of Mn, Fe, Ni and Cu Ions from wastewater using cow bone charcoal. *Materials* 3: 452–466.

Patel S, Han J, Qiu W, et al. (2015) Synthesis and characterisation of mesoporous bone char obtained by pyrolysis of animal bones, for environmental application. *Journal of Environmental Chemical Engineering* 3: 2368–2377.

Poinern GEJ, Senanayake G, Shah N, et al. (2011) Adsorption of the aurocyanide, $Au(CN)_2^-$ complex on granular activated carbons derived from macadamia nut shells – A preliminary study. *Minerals Engineering* 24: 1694–1702

Purkait MK, Gusain DS, DasGupta S, et al. (2005) Adsorption behavior of Chrysoidine dye on activated charcoal and its regeneration characteristics by using different surfactants. *Separation Science and Technology* 39(10): 2419–2440.

Reynel-Avila HE, Mendoza-Castillo DI and Bonilla-Petriciolet A (2016) Relevance of anionic dye properties on water decolorization performance using bone char: Adsorption kinetics. *Journal of Molecular Liquids* 219: 425–434.

Saucier C, Adebayo MA, Lima EC, et al. (2015) Microwave-assisted activated carbon from cocoa shell as adsorbent for removal of sodium diclofenac and nimesulide from aqueous effluents. *Journal of Hazardous Materials* 289: 18–27.

Tamanini CR, Motta ACV, Andreoli CV, et al. (2008) Land reclamation recovery with the sewage sludge use. *Brazilian Archives of Biology and Technology* 51(4): 643–655.

Tang QL, Zhu YJ, Duan YR, et al. (2010) Porous nanocomposites of PEG-PLA/calcium phosphate: Room-temperature synthesis and its application in drug delivery. *Dalton Transactions* 39: 4435–4439.

Tezcan Un U, Ates F, Erginel N, et al. (2015) Adsorption of disperse orange 30 dye onto activated carbon derived from Holm Oak (*Quercus ilex*) acorns: A 3k factorial design and analysis. *Journal of Environmental Management* 155: 89–96

The United Nations World Water Development Report 2015 (2015) *Water for a Sustainable World*. Paris: United Nations Educational, Scientific and Cultural Organization.

Tovar-Gomez R, Moreno-Virgen MR, Dena-Aguilar JA, et al. (2013) Modeling of fixed-bed adsorption of fluoride on bone char using a hybrid neural network approach. *Chemical Engineering Journal* 228: 1098–1109.

Walker G and Weatherley LW (2001) Adsorption of dyes from aqueous solution – The effect of adsorbent pore size distribution and dye aggregation. *Chemical Engineering Journal* 83(3): 201–206.

Wang L, Gruber S and Claupein W (2012) Optimizing lentil-based mixed cropping with different companion crops and plant densities in terms of crop yield and weed control. *Organic Agriculture* 2(2): 79–87.

Winter C, Caetano JN, Araújo ABC, et al. (2016) Activated carbons for chalcone production: Claisen-Schmidt condensation reaction. *Chemical Engineering Journal* 303: 604–610.

Zhao Y, Fang F, Xiao H, et al. (2015) Preparation of pore-size controllable activated carbon fibers from bamboo fibers with superior performance for xenon storage. *Chemical Engineering Journal* 270: 528–534.

Zúñiga-Muro NM, Bonilla-Petriciolet A and Mendoza-Castillo DI (2017) Fluoride adsorption properties of cerium-containing bone char. *Journal of Fluorine Chemistry* 197: 63–73.